Analysis of temperature-dependent mode transition in nanosized liquid crystal layer-coated long period gratings

Haimei Luo,[1,2] Xinwan Li,[1,*] Shuguang Li,[1] and Jianping Chen[1]

[1]State Key Laboratory of Advanced Optical Communication Systems and Networks, Shanghai Jiao Tong University, Shanghai 200240, China

[2]College of Physics and Communication Electronics, Jiangxi Normal University, Nanchang 330022, China

*Corresponding author: lixinwan@sjtu.edu.cn

Received 4 February 2009; revised 15 June 2009; accepted 6 August 2009; posted 7 August 2009 (Doc. ID 106840); published 24 August 2009

The cladding mode reorganization in high refractive-index (HRI)-coated long period gratings (LPGs) is theoretically analyzed and experimentally observed with the aim of exploring the sensitivity of the resonance wavelength to the change of the refractive index in a nanoscale overlay. Experimental results show that the transition between cladding modes and overlay modes occurs when the refractive index of the liquid crystal (LC) overlay is changed from 1.477 to 1.515 by increasing its temperature from 20 °C to 65 °C. The spectral tuning ability of LPGs coated with a HRI LC layer by electro-optic modulation on a LC layer is also demonstrated, and the maximum tuning range can reach approximately 10 nm by choosing a highly sensitive operating point in the transition region. © 2009 Optical Society of America

OCIS codes: 060.2330, 060.2340, 350.2770.

1. Introduction

In past years, in-fiber long period gratings (LPGs) have been widely investigated in the field of optical sensing and communications [1]. They have the ability to couple energy from the core mode to different cladding modes with the same propagation direction. The central attenuation wavelength of the LPGs is highly sensitive to the ambient refractive-index change [2,3] and, therefore, can be tuned by modulating the ambient refractive index by methods such as the thermo-optic effect [4], the electro-optic effect [5], or a combination of both methods.

Until now, most of the studies have concentrated on the analysis of the sensitivity to the surrounding medium refractive index (SRI) of the bare LPG [6,7]. The idea of coated LPGs with a thin high refractive-index (HRI) layer was first put forward by James *et al.* [8]. Then a detailed study was presented by Wang *et al.* [9] to investigate the sensitivity of LPGs when they are coated with nanometer thick film of a refractive index higher than that of silica. The results showed that resonant wavelength shifts that are due to similar film coating thickness and refractive-index values can be vastly different, depending on the coupled cladding modes. In the same year, a comprehensive theoretical and experimental investigation of the cladding modes reorganization in HRI layer-coated LPGs was reported by Cusano *et al.* [10]. Their analysis showed that by increasing the SRI, the transition from cladding to overlay modes occurred for a fixed overlay thickness and refractive index. As a matter of fact, changing the HRI could also lead to mode transition. The theoretical and experimental analysis presented by Del Villar *et al.* indicated that the highest sensitivity of the resonance wavelengths to the refractive-index change of the overlay can be optimized by selecting an overlay

0003-6935/09/250F95-06$15.00/0

refractive index that is close to that of the cladding of the LPG and reasonably close to the overlay thickness [11,12].

The effective refractive index of nematic LCs can be controlled by either the thermal or the electrical method [13]. LC is one of the attractive candidates as the coating material for potential applications in fiber optic sensing and in communications [14]. Therefore, adopting LC as the overlay material, we can use the phenomena of mode transition by controlling its temperature or use the external voltage to increase the sensitivity of the resonance wavelength of LPGs.

We designed an experiment to observe the cladding modes reorganization by changing the refractive index of the HRI layer and put forward a scheme for active electrical control and thermal stabilization tunable fiber gratings. Results of numerical simulations based on the coupled-mode theory are presented in Section 2. Experiments on the refractive index of LC with temperature, the thermal spectral tuning of LC-coated LPGs, and electrical tunability are presented in Section 3. Finally, conclusions are drawn in Section 4.

2. Theoretical Analysis

The coupling between the core mode and the copropagation cladding modes in a LPG acts as the spectral loss selection. The center wavelength λ_i of the ith attenuation band is given by the following phase-matching condition between the core and the cladding modes [15]:

$$\lambda_i = (n_{\text{co}} - n_{\text{cl}}^i)\Lambda, \tag{1}$$

where n_{co} and n_{cl}^i are the effective refractive indices of the core mode and the ith cladding mode, respectively. Λ is the grating period. The minimum transmission of the attenuation bands is governed by the expression [16]

$$T = \cos^2(k_i L), \tag{2}$$

where L is the length of the LPG and k_i is the coupling coefficient of the ith cladding mode, which is determined by the overlap integral of the core and cladding modes. The refractive-index sensitivity of the LPG arises from the dependence of the effective refractive indices of the cladding modes on the ambient refractive index. As the ambient index approaches the index of the LPG cladding, the sensitivity of the LPG increases sharply [6,17].

The structure of the coated LPG has four layers and the surrounding media is air as shown in Fig. 1. The analysis used the standard Corning SMF-28 optical fiber parameters: 0.14 numerical aperture, 0.36% refractive index difference [10], 125 and 8.2 μm cladding and core diameters, respectively. The HRI LC overlay has a refractive index of 1.47–1.55, which is close to the experimental testing refractive index [18,19], and with different thicknesses ranging between 600 and 900 nm. The effective indices of the cladding modes were retrieved as a function of the HRI.

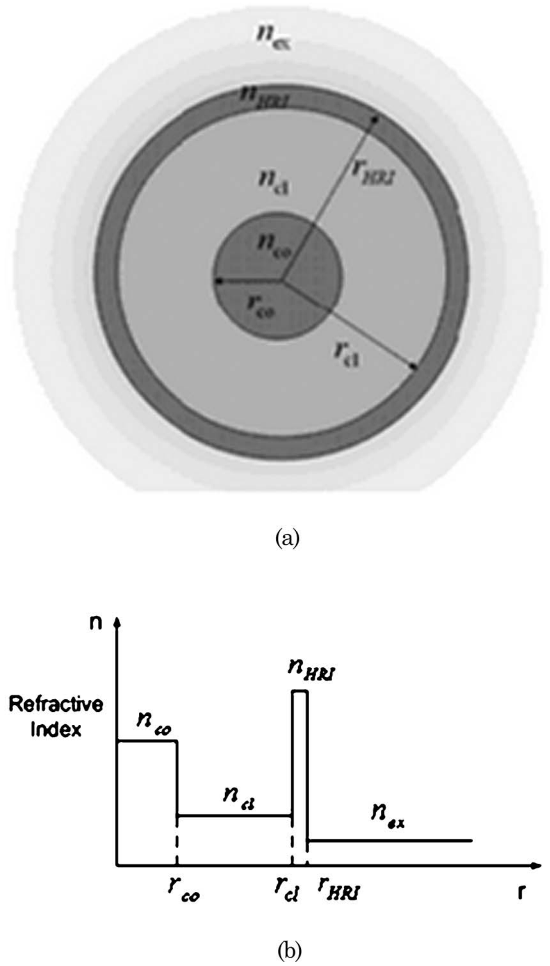

Fig. 1. (a) Illustrative schematic of a LPG with a nanometer thick thin-film coating and (b) index profile of the thin-film-coated LPG.

Figure 2(a) shows the effective index for each of the first six cladding modes as functions of the HRI for a 600 nm HRI overlay. As one can observe, the effective refractive index increases as the HRI increases until a critical point is reached. At this point, a significant shift in the effective index of cladding modes occurs. For a fixed overlay thickness, there is a value of the HRI that leads to the transition of the lowest-order cladding mode (higher effective index) to be guided within the overlay instead of cladding area only. As the lowest-order cladding mode moves to be guided within the overlay, a reorganization of the other cladding modes occurs.

Figures 2(b)–2(d) show the effective refractive index for a HRI overlay of 700, 800, and 900 nm, respectively. It can be seen that the transition point moves to a lower HRI as the overlay thickness increases.

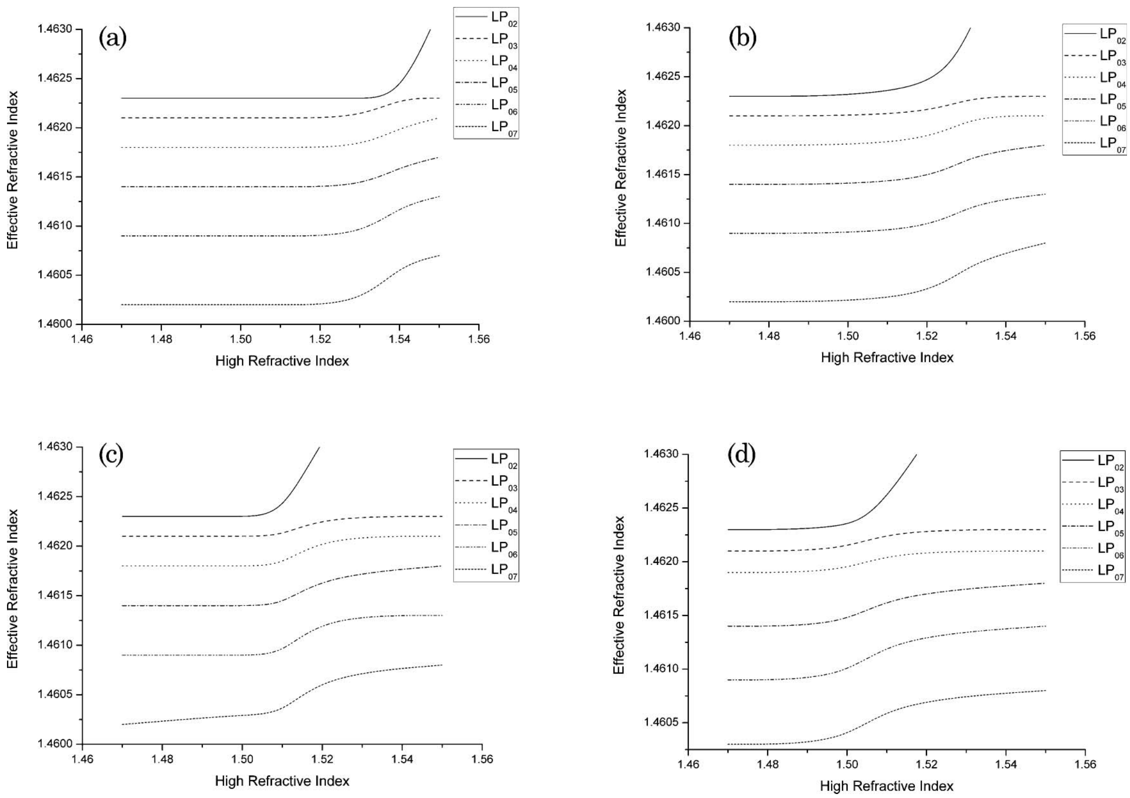

Fig. 2. Effective refractive index of the LP_{02}–LP_{07} cladding modes versus HRI-coated fiber with (a) 600, (b) 700, (c) 800, (d) 900 nm film.

3. Experimental Observation and Results

A. Temperature-Dependent Mode Transition in HRI-Coated LPGs

In this experiment, the LPG was fabricated using CO_2 laser irradiation on Corning SMF-28 fibers, with a grating period of 620 μm and a grating region of 50 mm. Attention bands were investigated in the range of 1400–1700 nm by use of a white light source in the 400–1800 nm wavelength range and an optical spectrum analyzer to record the spectral response of the device. The analysis was focused on the LP_{02} and LP_{03} cladding modes. With regard to the LP_{02} mode, we first measured the transmission spectrum of the bare LPG at temperatures ranging from 20 °C to 65 °C and determined that there is a slight wavelength redshift of approximately 1 nm.

Nanosized LC cladding material (MDA-98-3699, Merck Chemicals, Darmstadt, Germany) has a refractive index larger than that of silica. The coating process is as follows: We dipped a tampon in the LC and daubed it evenly on the fiber grating. The surface tension of the slimy LC makes it easy to coat uniformly. The thickness of the LC layer is controlled by the number of times it is dipped. Figure 3 shows CCD photographs of the bare and LC-coated LPG taken by an Olympus STM6 measuring microscope (Olympus Corporation, Tokyo, Japan). Figure 4 shows CCD photographs of approximate overlay thicknesses of (a) 400 nm and (b) 800 nm. A heater box was used to change the temperature of the LC from 20 °C to 65 °C.

Figure 5 shows the transmission spectrum of the ultrathin LC-coated LPG for different temperatures between 20 °C and 65 °C. In Fig. 5, the LP_{0i} mode has

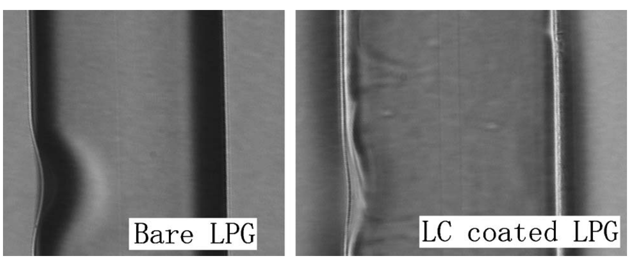

Fig. 3. CCD photographs of bare and LC-coated LPG.

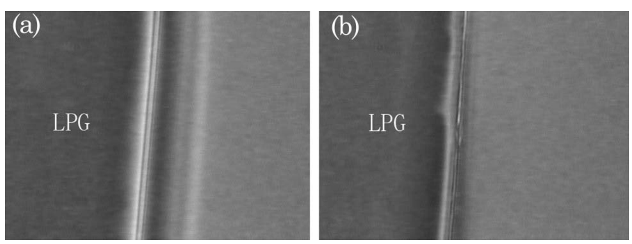

Fig. 4. CCD photographs reveal approximate overlay thicknesses of (a) 400 and (b) 800 nm.

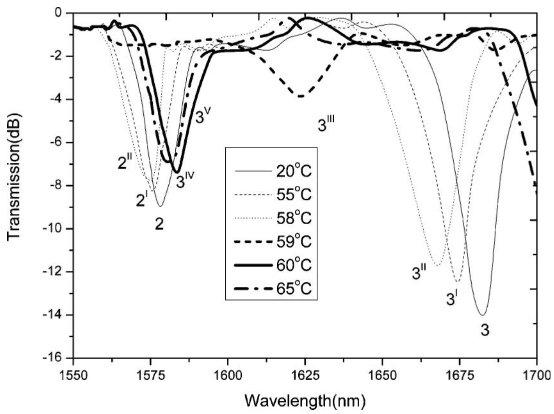

Fig. 5. Transmission spectra of an ultrathin HRI LC-coated LPG for different temperatures in the 20 °C–65 °C range.

been marked with i, i^j ($i = 2, 3, j = \mathrm{I, II, III, IV}$) for the different temperatures. As can be seen, a slight wavelength blueshift is achieved because of the increase in temperature from 20 °C to 58 °C. When the temperature reaches approximately 59 °C, a large wavelength shift in the attenuation band of the LP_{03} mode is observed. In particular, it is worth noting that the phenomenon of mode transition appears when the temperature is changed by only 2 °C, from 58 °C to 60 °C.

A clearer attenuation band shift is shown in Fig. 6. Outside the transition region, the center wavelength is shifted from 1579.7 to 1575.2 nm in the attenuation band of the LP_{02} mode and from 1687.5 to 1665.7 nm in the LP_{03} mode. Within the transition region, only the LP_{03} mode can be observed in the range of our investigation with its center wavelength shifting from 1665.7 to 1583.7 nm, which changes by the amount of 82 nm. We measured the temperature-dependent refractive index of the LC layer to clarify our experimental observations.

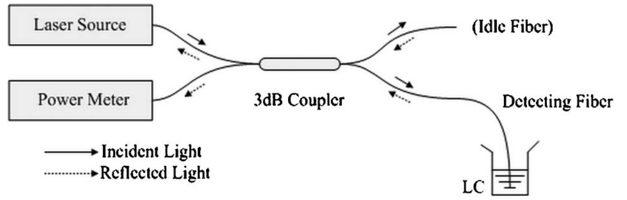

Fig. 7. Schematic diagram of the experimental setup for measurement of the refractive index of the LC.

B. Measurement of the Refractive Index of Liquid Crystal at Different Temperatures

The methods for measuring the refractive index of liquids can be classified into refractive techniques and reflective techniques including total reflection [20]. Figure 7 is a schematic diagram of the experimental setup, showcasing the efficient method developed by Pu *et al.* [21]. The detecting tip is immersed into air, water, and the LC under magnetic fields of different intensities, and the power of the reflected light is measured under each condition. Using the experimental data, the thermo-dependent refractive indices of the LC in the infrared can be calculated as shown in Fig. 8.

With the refractive-index data from our measurements, we calculated the center wavelength shifts theoretically [22], as shown in Fig. 9. It can be seen that the experimental results are in good agreement with the theoretical results. Figure 9(b) shows that the sensitivity enhancement to the HRI in the transition region was approximately six times the sensitivity outside the transition region for the LP_{03} mode. The center wavelength shifts over a small LC layer refractive-index range within the transition region, which means that one can choose this point as the highly sensitive operating point for sensor applications.

C. Electrical Spectral Tuning of LC-Coated Long-Period Gratings at the Highly Sensitive Operating Point

A simple scheme for active electrically controlled tunable fiber gratings is illustrated schematically

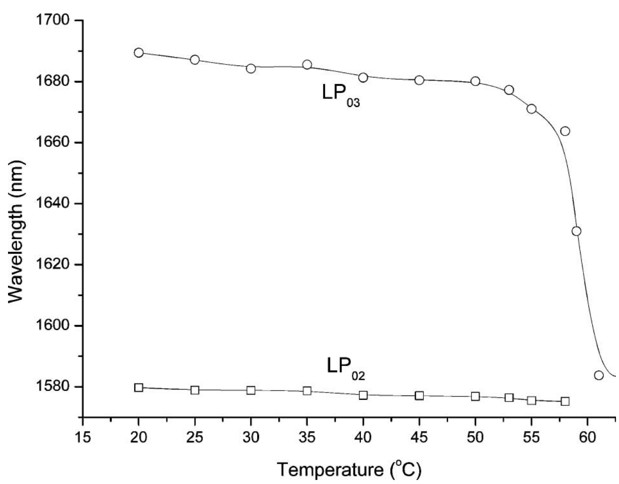

Fig. 6. Wavelength shift of LP_{02} and LP_{03} cladding modes for the LPG coated with a HRI layer versus temperature.

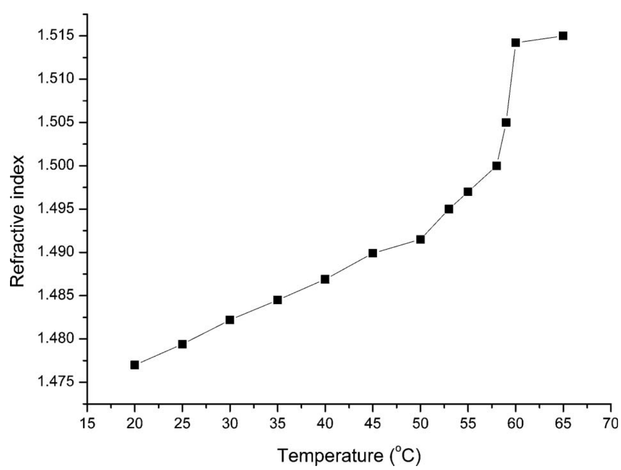

Fig. 8. Refractive index versus temperature (°C) of LC MDA-98-3699.

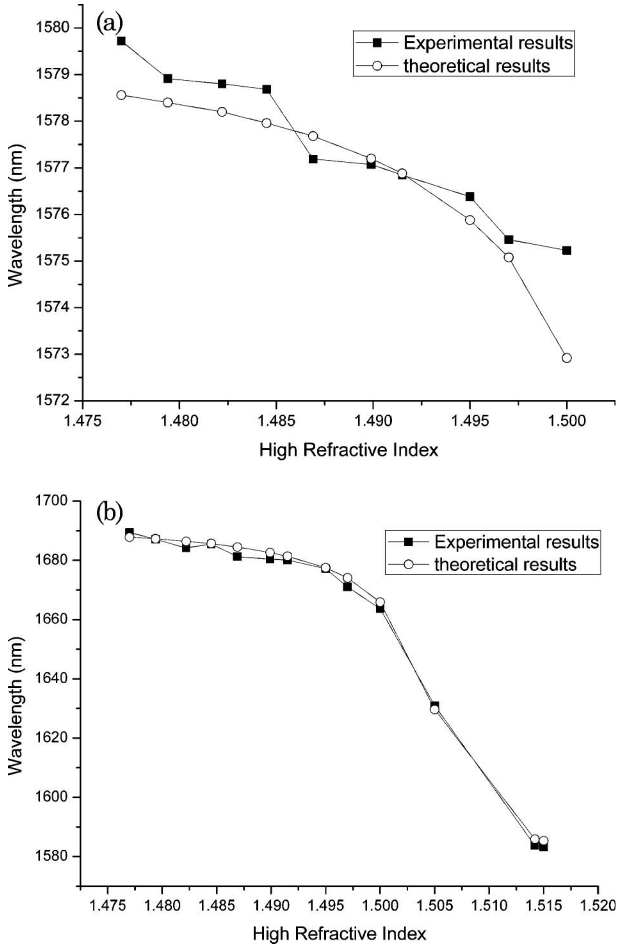

Fig. 9. Theoretical and experimental center wavelength dependence on HRI for (a) LP_{02} and (b) LP_{03}.

in Fig. 10. The LC-coated LPG is aligned between two substrates parallel to each other. The gap is maintained using 125 μm thick spacers. The external electric fields are applied using two parallel electrodes (200, 300, and 400 V were used in our experiment). The temperature is stabilized at 20 °C, 55 °C, 58 °C, 59 °C, 60 °C and 65 °C, respectively. Attention bands have been investigated in the range of 1500–1600 nm. Figure 11 shows the electrical spectra tunability of the LC-cladding LPG at different temperatures. $\Delta\lambda_{\text{res}}$ is the central wavelength shift. From Fig. 11 we can see that 60 °C is the most sensitive operating point for the LC used. The maximum tuning range is approximately 10 nm.

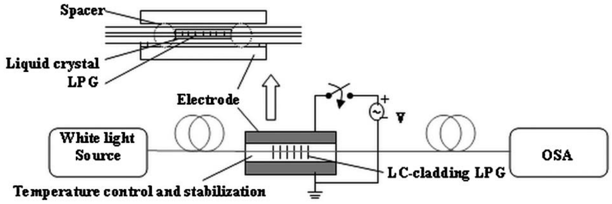

Fig. 10. Experimental setup and schematic of the LC cladding LPG.

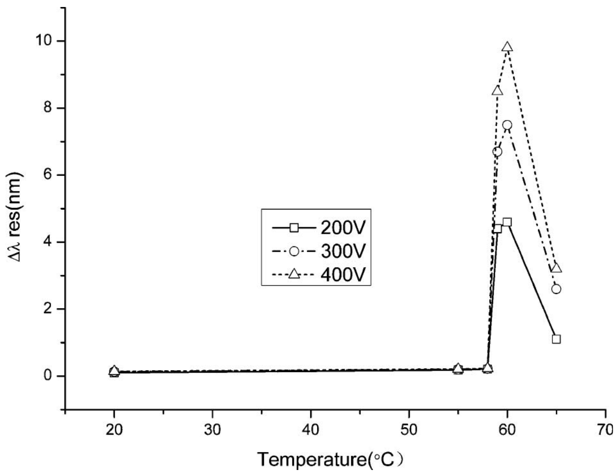

Fig. 11. Electrical spectra tunability of the LC cladding LPG at different temperatures.

4. Conclusions

The effect of the refractive-index change in the nanosized overlay on the resonant spectral tuning of the LPG has been theoretically and experimentally analyzed. Shifts of greater than 80 nm in the attenuation bands of the transmission spectrum can be obtained by changing the refractive index of the LC overlay through the thermo-optic effect. The sensitivity enhancement to the HRI in the transition region is approximately six times the sensitivity outside the transition region. A preliminary experimental demonstration shows that the electrical spectral tuning ability can be improved significantly by choosing an appropriate operating temperature.

This research was supported in part by the National Science Foundation of China (NSFC) (ID60877012), the 863 Project (ID2006AA01Z242 and 2007AA01Z275), the Dawn Program for Excellent Schools by the Shanghai Municipal Education Commission, the Science and Technology Commission of Shanghai (STCSM) project (09JC1408100), and the Key Disciplinary Development Program of Shanghai (T0102).

References

1. S. W. James and R. P. Tatam, "Optical fibre long-period grating sensors: characteristics and applications," Meas. Sci. Technol. **14**, R49–R61 (2003).
2. B. J. Eggleton, R. E. Slusher, J. B. Judkins, J. B. Stark, and A. M. Vengsarkar, "All-optical switching in long period fiber gratings," Opt. Lett. **22**, 883–885 (1997).
3. V. Bhatia, "Applications of long-period gratings to single and multi-parameter sensing," Opt. Express **4**, 457–466 (1999).
4. A. A. Abramov, A. Hale, R. S. Windeler, and T. A. Strasser, "Widely tunable long-period fibre gratings," Electron. Lett. **35**, 81–82 (1999).
5. Q. Chen, M. R. Lin, J. E. Lee, Q. M. Zhang, and S. Yin, "Nanocomposites with very large electro-optic effect and widely tunable refractive index," Appl. Phys. Lett. **89**, 141121 (2006).
6. H. J. Patrick, A. D. Kersey, and F. Bucholtz, "Analysis of the response of long period fiber gratings to external index of refraction," J. Lightwave Technol. **16**, 1606–1612 (1998).

7. T. Allsop, D. J. Webb, and I. Bennion, "A comparison of the sensing characteristics of long period gratings written in three different types of fiber," Opt. Fiber Technol. **9**, 210–223 (2003).
8. N. D. Rees, S. W. James, R. P. Tatam, and G. J. Ashwell, "Optical fiber long-period gratings with Langmuir–Blodgett thin-film overlays," Opt. Lett. **27**, 686–688 (2002).
9. Z. Wang, J. R. Heflin, R. H. Stolen, and S. Ramachandran, "Analysis of optical response of long period fiber gratings to nm-thick thin-film coatings," Opt. Express **13**, 2808–2813 (2005).
10. A. Cusano, A. Iadicicco, P. Pilla, L. Contessa, S. Campopiano, and A. Cutolo, "Mode transition in high refractive index coated long period gratings," Opt. Express **14**, 19–34 (2006).
11. I. Del Villar, I. R. Matias, and F. J. Arregui, "Long-period fiber gratings with overlay of variable refractive index," IEEE Photon. Technol. Lett. **17**, 1893–1895 (2005).
12. I. Del Villar, J. M. Corres, M. Achaerandio, F. J. Arregui, and I. R. Matias, "Spectral evolution with incremental nanocoating of long period fiber gratings," Opt. Express **14**, 11972–11981 (2006).
13. S. Yin, X. Zhu, and K.-W. Chung, "All-fiber all-optical tunable filter based on the combination of long period grating and photorefractive cladding layer," Proc. SPIE **4110**, 190–194 (2000).
14. A. Czapla, W. J. Bock, T. R. Wolinski, and P. Mikulic, "Towards spectral tuning of long-period fiber gratings using liquid crystals," in *21st Canadian Conference on Electrical and Computer Engineering* (IEEE Canada, 2008).
15. A.. M.Vengsarkar, P. J. Lemaire, J. B. Judkins, V. Bhatia, T. Erdogan, and J. E. Sipe, "Long-period fiber gratings as band-rejection filters," J. Lightwave Technol. **14**, 58–65 (1996).
16. V. Bhatia, "Properties and sensing applications of long-period gratings," Ph.D. dissertation (Virginia Tech, Blacksburg, Va., 1996).
17. B. H. Lee, Y. Liu, S. B. Lee, S. S. Choi, and J. N. Jang, "Displacements of the resonant peaks of a long-period fiber grating induced by a change of ambient refractive index," Opt. Lett. **22**, 1769–1771 (1997).
18. H. Luo, X. Li, S. Wang, X. Wang, and J. Chen, "Temperature dependent mode transition in high refractive index coated long period gratings," in *Proceedings of Asia Optical Fiber Communications and Optoelectronics Exposition and Conference* (Optical Society of America, 2008), paper SaE3.
19. H. Luo, X. Li, S. Wang, and J. Chen, "Temperature stabilized electrically tunable long period gratings coated with nanosized liquid crystal layer," in *Proceedings of OFC/NFOEC* (Optical Society of America, 2009), paper JThA22.
20. K. Schmid and A. Penzkofer, "Refractive-index measurements with a Pellin-Broca prism apparatus," Appl. Opt. **22**, 1824–1827 (1983).
21. S. Pu, X. Chen, Y. Chen, W. Liao, L. Chen, and Y. Xia, "Measurement of the refractive index of a magnetic fluid by the retroreflection on the fiber-optic end face," Appl. Phys. Lett. **86**, 171904 (2005).
22. T. Erdogan, "Cladding-mode resonances in short- and long-period fiber grating filters," J. Opt. Soc. Am. A **14**, 1760–1773 (1997).